Paper No. 003089
An ASAE Meeting Presentation

HYPERSPECTRAL IMAGE ANALYSIS FOR MEASURING RIPENESS OF TOMATOES

By

G. Polder, G.W.A.M. van der Heijden and I.T. Young*

Plant Research International, PO-Box 16,
6700 AA, Wageningen The Netherlands
E-mail: G.Polder@plant.wag-ur.nl,
G.W.A.M.vanderHeijden@plant.wag-ur.nl
*Delft University of Technology, Faculty of Applied Physics
Lorentzweg 1, 2628 CJ Delft, The Netherlands.
E-mail: young@ph.tn.tudelft.nl

Written for Presentation at the
2000 ASAE International Meeting
Sponsored by ASAE

Midwest Express Center
Milwaukee, Wisconsin
July 9-12, 2000

Summary:

The latest developments in optics and sensors allow imaging spectrometry: the creation of hyperspectral images, i.e. images with wavelength-specific measurements over a large part of the spectrum. In this study, hyperspectral images of several stages of ripeness of tomatoes were recorded and analyzed. The electromagnetic spectrum between 450 and 850 nm was recorded in 80 bands (every 5 nm).
Results show that hyperspectral images offer more discriminating power than standard RGB-images for discriminating ripeness stages of tomatoes, reducing the classification error of individual pixels from 40% to 7%. Using a reference tile, the images can be made invariant to the light source and even object geometry without losing discriminating power. This makes it possible to have comparable classification results under a large range of conditions.

Keywords:

Linear Discriminant Analysis, color constancy, multispectral, machine vision

1 Introduction

Traditionally, the surface color of tomatoes is a major decision factor for determining the ripeness of tomato fruits. A color chart standard has been specifically developed for the purpose of classifying tomatoes in twelve ripeness classes. Sometimes RGB-color cameras are used instead of the color chart. When comparing the ripeness of tomatoes in the RGB color-domain, however, we have to be aware of the strong dependency of the color on factors such as the spectral power distribution of the light source and object geometry. Van der Heijden et al [3] have shown that the color-information in hyperspectral images can be made invariant for these factors, hence providing a powerful alternative to RGB-color camera's.
In this study we want to compare hyperspectral images with standard RGB-images for classifying tomatoes in different ripeness classes using individual pixels.
The paper is organized as follows. First, we will describe imaging spectrometry and hyperspectral images. Next, we will show how the hyperspectral images can be transformed to images invariant to the light source and the object geometry. An experiment will then be described and the results will be given.

2 Imaging spectrometry

The ImSpector is a straight-axis imaging spectrograph that uses a prism-grating-prism (PGP) dispersive element and transmission optics [1,2]. The straight axis enhances the coupling with a lens/camera system with respect to most other imaging spectrographs which have a folded optical path. Off-axis configuration also causes astigmatism and other aberrations. With the PGP dispersive element, these problems are largely overcome due to the axial transmission spectrograph optics made possible by a holographically recorded transmission grating [5].
The ImSpector is available in several different wavelength ranges. Type V9, which is used in this experiment, has a spectral range of 430-900 nm and a slit size of 50 µm resulting in a resolution of 5nm.The ImSpector uses one axis of the CCD-chip as the spatial axis and the other as the spectral axis. Therefore, a single camera frame contains a one-dimensional line of the object. To record a spatial two-dimensional image, the object has to be moved perpendicular to the optical axis of the camera. For this we use a linear translation table.

2.1 Color Constancy

Van der Heijden et al [3] show that spectral images obtained with the ImSpector can be made independent of the light source (*color constant*) using the Shafer [6] reflection model and dividing the reflection values of the spectral image by the spectral power distribution function of the light source as obtained by spectral reflection of a nearly perfect white object. We have used a white tile of PTFE-plastic with a spectral reflectance of over 0.98 from 400 to 1500 nm (TOP Sensor Systems WS-2). The color constant images can be calculated using equation (1), where X_λ is the color constant reflection value at wavelength λ , I_λ is the original measured spectral reflection value, B is the pixel value of the camera in the dark (black reference) and W_λ is the reflection value at wavelength λ of the white reference tile.

$$X_\lambda = \frac{I_\lambda - B}{W_\lambda - B} \tag{1}$$

Note that the spectral power distribution of the light source is unimportant as long as it contains all wavelengths of the visible light in a sufficient amount.

2.2 Normalization

The color constant image is independent of the light source, but these images are not invariant to influences of object geometry such as shadows. Assuming matte surfaces, however, van der Heijden et al[3] have shown that the images can also be made invariant to object geometry. Normalizing the spectral values X_λ according to equation (2) results in a spectral value Y_λ which is independent of the illumination spectral power distribution, illumination direction and object geometry.

$$Y_\lambda = \frac{X_\lambda}{\sum_\lambda X_\lambda} \tag{2}$$

3 Experiment

3.1 Image recording of tomatoes

Four tomatoes (Capita F1 from De Ruiter Seeds, Bergschenhoek, Netherlands) in four different ripeness stages were harvested. At harvest, the ripeness stages were 1, 5, 7 and 12, as defined by a color chart standard commonly used by breeders. Each day over a time period of 12 days, a color RGB image and a spectral image were taken of the four fruits on a black velvet background. Figure 1 shows the time series of RGB images.

A Sony DX-950P 3-CCD camera was used to record the images. The light source consisted of high frequency fluorescent daylight tubes (6500 K). The frame grabber used was a Matrox Meteor RGB.

The spectral images were recorded using 1000 W Tungsten halogen light as light source, a Hitachi B/W camera with an ImSpector V9 and a NIKON 55 m lens. The frame grabber used was a Matrox Meteor II. The translation table used to move the object with respect to the camera is from Lineartechniek and is driven by a programmable microstepping motor driver (Ever Elettronica, Italy).

Full size hyperspectral images are large, with a spatial resolution in the x-direction of 768 pixels and a spectral resolution of 512 pixels. If the same spatial resolution of 512 pixels in the y-direction would be used, obtained by movement of the translation table, a single hyperspectral image would be 20 MB large. Due to limitations in optics, such a spectral image is oversampled and binning can be used to reduce the size of the image. The software allows binning of the image separately in both the spatial and the spectral axes during build-up of the image. The binning factor in the spatial x-axis was 2. In the spectral axis a binning factor was chosen such that a spectral resolution of 96 bands (from 430-900 nm) remained. The low radiation from the light source in the lower part of the band (between 430 and 450 nm) and the low sensitivity of the CCD camera in the lower and upper parts of the spectrum produced a low signal to noise ratio in these parts of the spectrum. We, therefore, reduced the spectrum to 80 bands, from 450-850 nm. The step size of the stepper table was chosen to match the binned spatial resolution in the x-direction. The resulting images have a spatial dimension of 256x256 square pixels (resolution 0.5mm/pixel) and a spectral dimension of 80 bands (about 5 MB).

The software to control the stepper table and frame grabber, to construct the hyperspectral images and to save and display them has all been locally developed in a single, integral computer program written in Java.

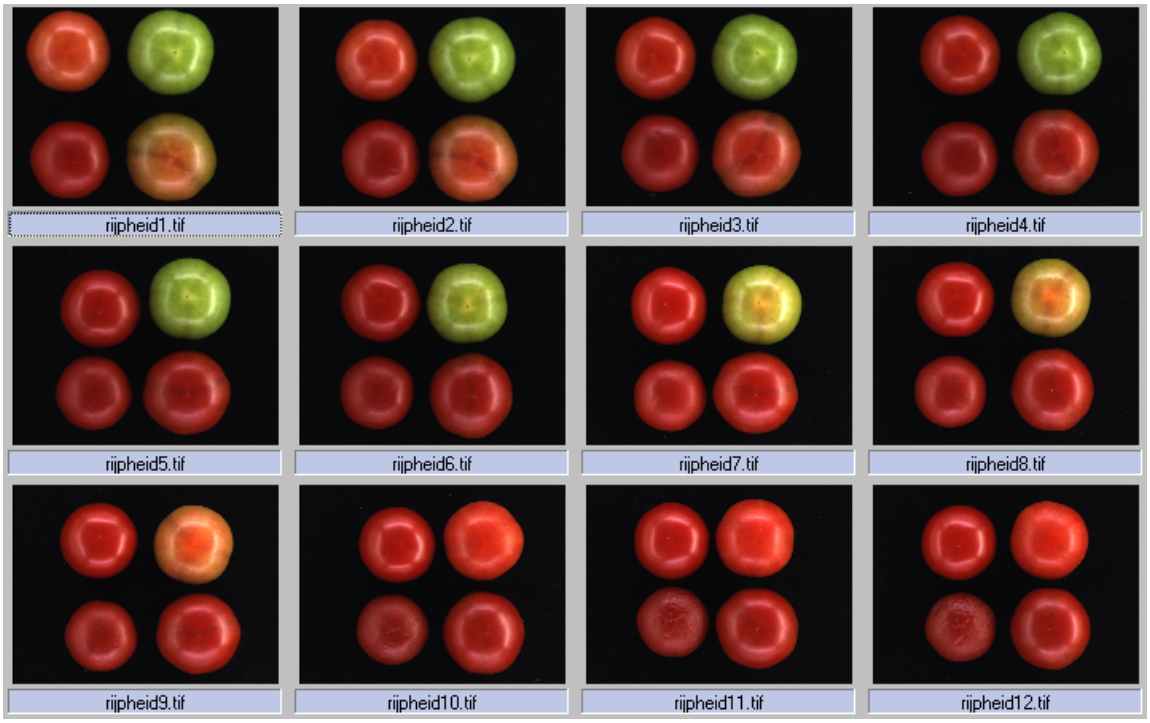

Figure 1: Time series of four tomatoes from four different initial ripeness stages. Each sub image shows four tomatoes. In the first image (rijpheid1.tif), the upper left tomato has initial ripeness stage 7, the upper right tomato stage 1, the lower left stage 12 and the lower right stage 5.

3.2 Data analysis

Data analysis is done in the following steps. First some image preprocessing is performed as described in the section below. The preprocessed images are then analyzed with principal component analysis (PCA) and Linear discriminant analysis (LDA). All analyses are done using Matlab (The Mathworks Inc.) and the Matlab PRTools toolbox (Faculty of Applied Physics, Delft University of Technology). The LDA is calculated in Genstat (IACR, Rothamsted, UK).

3.2.1 Image preprocessing

To separate the tomatoes from the background and handle each tomato image as a separate object, a threshold is performed on the intensity image of the RGB and spectral images. The intensity image is calculated as the sum of the R, G and B plane of the RGB-image and the sum of the different band planes for the spectral image. The binary image that is obtained is labeled, giving the locations of the four fruits in each image. As can be seen in figure 1 the images contain high intensity regions, caused by specular reflection of the illumination source at the tomato surface. A similar specular reflection can be observed in the spectral images. These specular regions are discarded by thresholding the intensity image. The threshold value applied is 1.1 * the grey value median of the image. Using an eight connected binary closing, single pixels are removed and a labeled mask image is calculated with one label for each tomato object, discarding the specular regions.

3.2.2 Principal component analysis

To compare the discriminating power of the spectral images with that of RGB images, we reduced the number of bands to three. For this, we use principal component analysis (PCA). PCA finds orthogonal linear combinations of a set of features (spectral bands) that maximize the variation contained within them, thereby displaying most of the original variation in a smaller number of dimensions. It operates on the sums of squares and products matrix, formed from the original features. A random set of 50 pixel spectra from each labeled tomato object is selected. This is done for tomato 2 (initial ripeness class 5 at harvest) for the first 5 time steps. Using PCA, the original spectrum vector of 80 data points is hence reduced to a vector of only 3 data points

3.2.3 Linear discriminant analysis

Linear discriminant analysis (LDA) is a technique that maximizes the ratio of the between-classes variance over the within-class variance. A detailed description of LDA can be found in the literature including Ripley [4]. In contrast to the PCA, the LDA needs to be trained with *a priori* information to calculate the within-class and between-class variances. We counted each labeled tomato as a separate ripeness stage. From the similarly labeled tomato objects, 250 (pixel) spectra were randomly selected to form a learning set for the LDA. From the remaining spectra, 250 spectra were randomly chosen to form the test set. The LDA consists of Linear Discriminant Functions (LDF) which map the original 80 features to a new feature, often referred to as canonical variate.
To compare the power of spectral images with that of RGB images for ripeness classification, we compared the LDA of the RGB-images with the LDA of the original (raw) spectral images, the color constant spectral images (see eq. (1)), and the normalized spectral images (see eq. (2)). To reduce the number of classes, only the tomatoes with initial ripeness class 5 (lower right) are used during the first 5 days (time steps).
After learning the LDA of each spectrum or RGB triple, the test sets are classified.

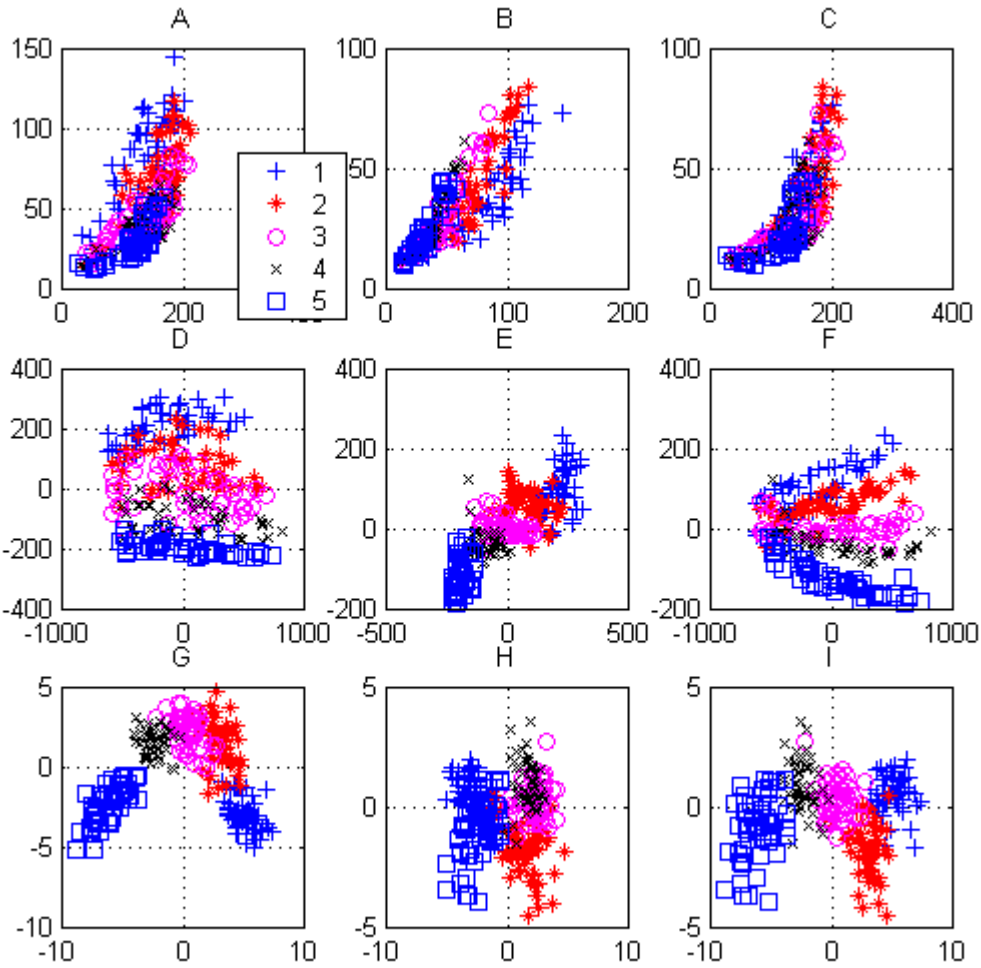

Figure 2: Scatterplot of the RGB points of the color images and the PCA and LDA analysis of the raw spectral images. Depicted is: A=R.G, B=R.B and C=G.B, D=first against second PCA component, E= second against third, F= first against third. G=first against second canonical variate, H= second against third, and I=first against third. Classes 1-5 represent the ripeness stages of tomato 2 (lower right of figure 1) during the first five days after harvest.

4 Results

Scatterplots were made of randomly selected test sets with 50 points per object, from the original RGB triplets, the first 3 PCA components of the spectral images and the LDA mapping to 3 canonical variates (figure 2). From these plots, it is clear that the different time stages of the tomato in the RGB domain show considerable overlap. The overlap in the PCA and LDA domain of the spectral images is considerably reduced. Due to the reduction of variation within classes, the classes in the LDA domain are much more concentrated.

The result of the LDA classification of ripeness stages of RGB images against the actual stages is tabulated in table 1. The error rate is 40 %. In table 2 the result of the LDA classification of the raw spectral images is shown, the error rate is 7%. Table 3 shows the LDA classification of the color-constant, spectral images; the result is exactly the same as with the raw spectral images. In table 4 the result of the LDA classification of normalized color constant spectral images is tabulated. The results differ slightly from the color-constant and raw images, but the error rate remains the same. To compare the classification power of the LDA with the

PCA, we did a LDA classification on the first 3 PCA components of the raw spectral images. The error rate is 24% (Table 5).

LDA RGB Actual	**1**	**2**	**3**	**4**	**5**
1	204	43	0	3	0
2	49	132	42	26	1
3	1	44	126	42	37
4	0	3	45	111	91
5	0	0	11	58	181

Table 1: Cross table of the actual ripeness stage against the ripeness stage determined with the LDA on a test set of the RGB images. Error rate: 40%

Raw spectra Actual	**1**	**2**	**3**	**4**	**5**
1	237	10	3	0	0
2	3	229	18	0	0
3	0	12	224	14	0
4	0	2	8	240	0
5	0	0	0	13	237

Table 2: Cross table of the actual ripeness stage against the ripeness stage determined with the LDA on a test set of the raw spectral images. Error rate: 7 %

Color constant Actual	**1**	**2**	**3**	**4**	**5**
1	237	10	3	0	0
2	3	229	18	0	0
3	0	12	224	14	0
4	0	2	8	240	0
5	0	0	0	13	237

Table 3: Cross table of the actual ripeness stage against the ripeness stage determined with the LDA on a test set of the color-constant spectral images. Error rate: 7 %

Normalized Actual	**1**	**2**	**3**	**4**	**5**
1	241	6	3	0	0
2	5	231	14	0	0
3	0	11	221	18	0
4	0	1	15	234	0
5	0	0	0	9	241

Table 4: Cross table of the actual ripeness stage against the ripeness stage determined with the LDA on a test set of the normalized color constant spectral images. Error rate: 7 %

PCA Actual	**1**	**2**	**3**	**4**	**5**
1	209	41	0	0	0
2	38	158	54	0	0
3	0	50	160	40	0
4	0	0	48	202	0
5	0	0	0	31	219

Table 5: Cross table of the actual ripeness stage against the ripeness stage determined with the LDA on a test set of the first 3 PCA components of the raw spectral images. Error rate: 24 %

5 Discussion

A RGB color camera is frequently used for ripeness sorting. In this paper we showed that considerable errors can occur when classifying small differences in ripeness stage using RGB images. Spectral images are more suitable for classifying ripeness stage but these images are very large. Using Principal Component Analysis (PCA) and Linear Discriminant Analysis (LDA), the number of spectral bands is reduced while maintaining most of the relevant information as described by the variations. From table 5 we learn that the LDA performs better than the PCA but we have to take into account that the PCA is an unsupervised technique whereas the LDA is based on *a priori* information. Hyperspectral images allow us to become independent of the light source and, after normalization, of object geometry as well.
The results of the LDA on the raw spectral images are identical to those of the LDA on the color-constant images. This can be expected, since in eq. (1) W_λ and B are constants for every λ. As a result X_λ is a linear transformation of I_λ and LDA is invariant for linear transformations. W_λ and B can change when new calibrations are performed, but this experiment is based on one calibration. If the spectral power distribution of the light source changes, W_λ is not a constant anymore. In that case the color-constant images are to be preferred since they remain independent of the light source as long as the light source is regularly measured. This can be realized by recording a small piece of white reference material in every image.
The LDA on the normalized spectral images performed as well as the LDA on the color constant images. This has the advantage that we are now also independent of object geometry: observed color has become independent of the surface normal, the angle of incident light, and the angle of view. When using normalized images, the color is independent of these factors and also of shading effects, as long as sufficient light is still present.
In the experiment described, the learning set and the test set were taken from the same tomatoes. In the near future we plan to repeat the experiment using a large set of tomatoes in different ripeness stages. We will also study whether it will be possible to measure non uniform ripening of individual fruits.

We have only looked at the ripening of tomatoes as an overall process in time. However, ripening is a combination of processes including the breakdown of chlorophyll and build-up of carotenoids. Chlorophyll and carotenoids have specific, well-known reflection spectra. The reflectance spectrum of live plant material is a combination of the individual spectra of specific compounds including chlorophyll and carotenoids. Using knowledge of the known spectral properties of the main constituting compounds, it may be possible to unravel the spectrum of the live plant material and separately measure the specific compounds. By combining pattern recognition and image analysis techniques with biochemical and physiological methods, it may be possible to assess the specific compounds in a non-destructive and rapid way in live plant tissue. This offers new possibilities for a variety of applications such as sorting, quality control, and breeding. The long term aim of the project is to develop methods for measuring the amount of compounds in a way that preserves the spatial information.

References

[1] Herrala Esko, Okkonen Jukka: *Imaging spectrograph and camera solutions for industrial applications*, International Journal of Pattern Recognition and Artificial Intelligence Vol.10 No.1 (1996) 43-54

[2] Hyvärinen Timo, Herrala Esko and Dall'Ava Alberto: *Direct sight imaging spectrograph: a unique add-on component brings spectral imaging to industrial applications*, SPIE symposium on Electronic Imaging, Vol. 3302 (1998)

[3] Van der Heijden, G.W.A.M., G. Polder & T. Gevers. *Comparison of multispectral images across the Internet*. Proceedings of SPIE-Internet Imaging. Vol 3964: 196-206. (2000)

[4] Ripley, B.D. *Pattern Recognition and Neural Networks.* Cambridge University Press. (1996)

[5] Pollet, P, F. Feyaerts, P. Wambacq and L. Van Gool. *Weed Detection based on Structural Information using an Imaging Spectrograph*. Proceedings of the 4th International Conference on Precision Agriculture, Minnesota, July 1998.

[6] Shafer, S.A. *Using color to separate reflection components*, COLOR Res. Appl. 10(4). pp 210-218, 1985.